

Analytics of Longitudinal System Monitoring Data for Performance Prediction

Ian J. Costello
Google, Inc.
Mountain View, USA
ianjc@google.com

Abhinav Bhatele
Department of Computer Science,
University of Maryland
College Park, USA
bhatele@cs.umd.edu

Abstract—In recent years, several HPC facilities have started continuous monitoring of their systems and jobs to collect performance-related data for understanding performance and operational efficiency. Such data can be used to optimize the performance of individual jobs and the overall system by creating data-driven models that can predict the performance of jobs waiting in the scheduler queue. In this paper, we model the performance of representative control jobs using longitudinal system-wide monitoring data and machine learning to explore the causes of performance variability. We analyze these prediction models in great detail to identify the features that are dominant predictors of performance. We demonstrate that such models can be application-agnostic and can be used for predicting performance of applications that are not included in training.

Index Terms—performance variability, data analytics, machine learning, prediction models

I. MOTIVATION

Run-to-run variability in the performance of parallel codes running on production high performance computing (HPC) platforms is a real problem [1]–[3]. Figure 1 shows the varying performance of two HPC applications, Algebraic Multigrid (AMG) and MIMD Lattice Computation (MILC), in spite of running the same executable and input in each job. This variability occurs either due to operating system noise impacting compute regions in the code or due to varying load on shared resources such as the network or filesystem because of changing workloads on the system. There are several ways to mitigate the former but diagnosing and mitigating the impact of the latter is still a challenge on many HPC systems.

Sharing of network or filesystem resources by all concurrently running jobs leads to uneven resource usage over time, which can impact performance reproducibility. For individual HPC users, reducing performance variability leads to more predictable performance, faster scientific results, and reduced allocation costs. At a system level, better performance of individual jobs leads to both energy savings and higher overall job throughput.

In recent years, several HPC facilities have started continuous monitoring of their systems and jobs to collect performance-related data for understanding performance and operational efficiency [4]. Analyzing such data and using it for data-driven modeling can facilitate understanding the causes

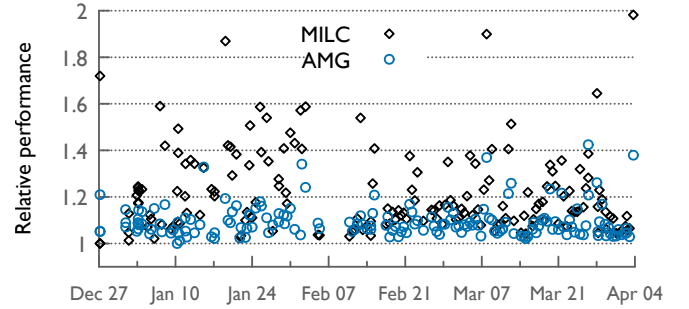


Fig. 1. Variability in the performance of 128-node AMG and MILC jobs on different days (on Cori at NERSC).

of performance variability, forecasting performance, and in providing insights that can translate into actions for correcting inefficient behavior. For example, an intelligent software stack can use modeling to predict the runtime of jobs waiting in the scheduler queue and use those models to adapt scheduling decisions to mitigate performance variability [5].

In this paper, we analyze longitudinal system monitoring data to explore the causes of performance variability in certain *control* jobs. The monitoring data is collected by the Lightweight Distributed Metric Service (LDMS) [6], [7] on Cori, a ~ 30 Pflop/s Cray XC40 system (recently retired) at NERSC. Analyzing system-wide monitoring data gives us a global view of the system, a perspective which users running individual jobs do not have. Separately, we also run some control jobs on Cori to document the impact of varying resource usage on application performance. Our goal is to use information about the system state before a job starts executing to create a model that can predict the performance of future jobs based on the system state at that time.

LDMS is becoming more prevalent on HPC systems, specially at Department of Energy centers and even some NSF centers. The Blue Waters machine at NCSA has used LDMS for a long time. ALCF/ANL, LC/LLNL, and NERSC/LBL are all using LDMS for collecting monitoring data on their clusters. While specific metrics/features may be different depending on the compute and networking hardware, the methodology developed in this paper should translate without

much effort to other centers running LDMS.

We use machine learning, specifically regression models, to model the execution time of jobs in terms of several network related hardware counters gathered by LDMS. We use these models to understand which hardware counters are strong predictors of performance, in other words, indicators of performance degradation. We demonstrate that our data-driven modeling approach that uses past system state is successful in performance prediction of unseen data – i.e. new jobs waiting in the scheduler queue.

Our work makes the following important contributions:

- We create a pipeline to process, filter and aggregate large-scale system-wide monitoring data to make it suitable for consumption by ML models.
- We develop ML-based regression models that can predict the performance of unseen jobs using past system state.
- We analyze feature importances in different models to identify strong predictors of performance degradation and show how lightweight monitoring of these counters can lead to powerful insights prior to job execution.
- We demonstrate that such models can be application-agnostic and can be used for predicting performance of applications that are not included in the training data.

II. BACKGROUND AND RELATED WORK

In this section, we provide background on sources of performance variability and related work. We first briefly describe the dragonfly network deployed in Cori (Cray XC40), which is used for experiments in this paper. The Cray XC40 system uses the Aries router to create a dragonfly network topology [8]. The Aries router has 48 ports that are used to connect to compute nodes and other routers on the network (see Figure 2). Eight ports referred to as processor tiles are used to connect to four compute nodes. The remaining 40 ports are referred to as router tiles and are used to connect to other routers. 96 Aries routers are connected in a 16×6 rectangular grid to form a logical group. In a group, each router is directly connected to all other routers in its row and all other routers in its column. The remaining ports are used for global links which connect to routers in other groups throughout the system.

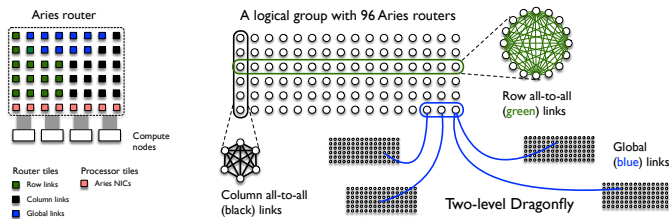


Fig. 2. Network ports classified into router and processor tiles on the 48-port Aries router (left) and a multi-group dragonfly system constructed using the Aries router as a building block (right).

A. Resource Management and Sources of Variability

On most HPC systems, compute nodes are dedicated to individual jobs but the global network and filesystem are shared

by all concurrently running jobs. Moreover, job schedulers assign any available nodes to “ready” jobs in the queue without regard to the nodes’ location in the physical network topology. Cray dragonfly-based systems are no exception to this. There are no guarantees provided by the job scheduler as to the “compactness” of a job allocation. Hence, a job may share routers and groups with other jobs.

In principle, the compactness of a job should have no bearing on its communication or overall runtime because adaptive indirect routing deployed on dragonfly networks should distribute traffic evenly over all global links [9]. However, in practice, significant performance variability can be observed when the same executable is run on a dragonfly system repeatedly. This paper primarily considers such effects of network traffic on variability. Traffic on the network consists of within-job communication, for example MPI messages, and traffic from/to the filesystem during input/output (I/O) operations. Even in the absence of OS noise, this resource sharing by concurrently running jobs can have a significant performance impact.

B. Related Work

Performance variability refers to the variation in the execution time of an application executable with the same input parameters across multiple executions. Several studies have established the significant differences in performance between identical executions of the same HPC job [1]–[3], [10], [11]. Petrini et al. [1] highlight the role of operating system daemons in creating noise and in degrading application performance.

Research on collecting system data for analysis and forecasting is not new. More than 25 years ago, Wolski et al. [12] developed a system called the Network Weather Service (NWS) to estimate CPU usage and throughput of network traffic based on system state and statistical models. In 2005, Skinner et al. [13] highlighted the impact of cross-application contention and parallel filesystem interference on the NERSC IBM SP system (Seaborg).

In recent years, HPC researchers have begun to explore the breadth of historical data available due to comprehensive data gathering at HPC facilities [4], [14]. Lockwood et al. [4] discuss performance variations due to varying load on the I/O sub-system. Tuncer et al. [14] perform classification and detection of anomalous performance based on Aries counters. They use machine learning combined with system data, but primarily focus on diagnosing anomalies in compute node health and not performance of jobs. Hoppe et al. [15] demonstrate a data pipeline for LDMS to classify anomalies on a smaller scale than the system that we use in this paper (52 versus 12,076 compute nodes). Agelastos et al. [7] create a HPC system profiler to explain the performance variability of applications across different HPC systems.

Jha et al. [16] investigate the relationship between overall during-run network congestion and performance. Chunduri et al. [17] measure and attribute runtime variation to runtime system state. However, they primarily focus on single node variation using data from the same time period as the execution

TABLE I
DESCRIPTION OF RAW NETWORK HARDWARE PERFORMANCE COUNTERS GATHERED BY LDMS. THESE RAW COUNTERS ARE AGGREGATED WITHIN A ROUTER ACROSS NETWORK TILES OR PROCESSOR TILES.

Raw counter name	Description
AR_RTR_INQ_PRF_INCOMING_FLIT_VCv	Number of flits received on virtual channel v of a router tile (8 counters)
AR_RTR_INQ_PRF_INCOMING_PKT_VCv	Number of cycles stalled on a virtual channel v of a router tile (8 counters)
AR_RTR_INQ_PRF_ROWBUS_STALL_CNT	Total number of cycles stalled on a router tile
AR_NL_PRF_REQ_NIC_n_TO_PTIRES_FLITS	Number of NIC request flits from NIC n to all processor tiles
AR_NL_PRF_REQ_PTIRES_TO_NIC_n_FLITS	Number of NIC request flits from all processor tiles to NIC n
AR_NL_PRF_RSP_NIC_n_TO_PTIRES_FLITS	Number of NIC response flits from NIC n to all processor tiles
AR_NL_PRF_RSP_PTIRES_TO_NIC_n_FLITS	Number of NIC response flits from all processor tiles to NIC n
AR_NL_PRF_REQ_NIC_n_TO_PTIRES_STALLED	Number of clock cycles requests from NIC n have stalled to all processor tiles
AR_NL_PRF_REQ_PTIRES_TO_NIC_n_STALLED	Number of clock cycles requests from all processor tiles have stalled to NIC n
AR_NL_PRF_RSP_NIC_n_TO_PTIRES_STALLED	Number of clock cycles responses from NIC n have stalled to all processor tiles
AR_NL_PRF_RSP_PTIRES_TO_NIC_n_STALLED	Number of clock cycles responses from all processor tiles have stalled to NIC n

of a job. In [18], Chunduri et al. perform a thorough analysis and build regression models of job performance using network counters from during the run. Bhatele et al. [3] analyze data from during a job's execution and use regression models to analyze per-job data combined with system data to predict the overall performance and per time step performance of individual jobs. However, they use data from when a job is running and in this work, we use only system data strictly before a job's execution. Nichols et al. [5] train machine learning models using system monitoring data to predict the occurrence of variation, and use these models in a job scheduler to alter scheduling decisions. Our proposed pipeline and analysis remain relevant across different HPC systems and routers as our work can be applied to any system with LDMS data collection.

III. DATA DESCRIPTION

We now describe the system-wide data obtained from LDMS, and control jobs' data used for training ML models. The data was gathered on Cori, a Cray XC40 system at NERSC. Cori features 12,076 compute nodes across 34 groups; of these 9,668 nodes are powered by 68-core Intel Xeon Phi Knights Landing (KNL) processors [19].

A. Longitudinal System Monitoring Data

LDMS enables system administrators to collect system-wide data on HPC clusters at a configurable frequency from a few seconds to minutes. We now describe the subset of the LDMS data that we use in our analysis and the processing of this data to facilitate ingestion by machine learning models.

Raw LDMS Data: Each Aries router has a multitude of hardware counters that track various network events across each router and processor tile [20]. The raw LDMS data collected on Cori consists of a subset of these hardware counters, collected every second for each of the 48 network tiles, across all 2890 routers on the system. In this paper, we consider a subset of these counters (see Table I, column 1) that we believe to be important indicators of network congestion.

Data Extraction from Time Series: The raw LDMS counter data is essentially a time series. Since we are interested in

predicting the performance of unseen jobs using system data from the recent past, we decided to extract data for the last five minutes prior to the beginning of execution of each control job (described in Section III-C). For each control job, we filter the time series by only looking at the last five minutes prior to the start time of a job and extracting the change in counter values (see Figure 3). For each job, this gives us a table of key-value pairs that are the previously identified network counters and the change in their values in the last five minutes. This data is available for each router and network tile on the system.

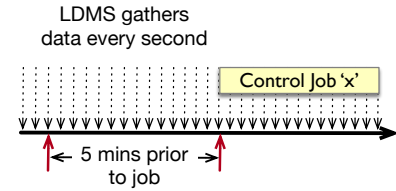


Fig. 3. LDMS data five minutes prior to job start is used as input to train the machine learning models.

LDMS is becoming more prevalent on HPC systems, specially at Department of Energy centers and even some NSF centers. The Blue Waters machine at NCSA has used LDMS for a long time. ALCF/ANL, LC/LLNL, and NERSC/LBL are all using LDMS for collecting monitoring data on their clusters. While specific metrics/features may be different depending on the compute and networking hardware, the methodology developed in this paper should translate without much effort to other centers running LDMS.

B. Reduction in Data Dimensionality

The resulting data extracted from the raw time series is still extremely high-dimensional because the counter values are per network tile (port) and per router. We perform aggregations of this data along different axes to get the data in final form:

Reducing Per Tile Data: We begin by performing reductions within each individual router. Each 48-port Aries router contains 40 router tiles or ports that connect to other routers and the remaining eight processor tiles or ports connect to the compute nodes on that router. The aggregation across

TABLE II
DESCRIPTION OF DERIVED COUNTERS USED FOR MODELING. COLORS IN THE LEFT COLUMN PROVIDE A MAPPING OF DERIVED FEATURES IN THIS TABLE TO RAW FEATURES IN TABLE I.

Derived counter name	Abbreviation	Description for interpreting counter
AR_RTR_INQ_PRF_INCOMING_FLIT_REQ	RT_FLIT_REQ	Total number of request flits received on a router tile
AR_RTR_INQ_PRF_INCOMING_FLIT_RSP	RT_FLIT_RSP	Total number of response flits received on a router tile
AR_RTR_INQ_PRF_INCOMING_PKT_REQ	RT_PKT_REQ	Total number of cycles requests stalled on a router tile
AR_RTR_INQ_PRF_INCOMING_PKT_RSP	RT_PKT_RSP	Total number of cycles responses stalled on a router tile
AR_RTR_INQ_PRF_INCOMING_FLIT_ROW	RT_FLIT_ROW	Total number of flits received on all row links of a router
AR_RTR_INQ_PRF_INCOMING_FLIT_COL	RT_FLIT_COL	Total number of flits received on all column links of a router
AR_RTR_INQ_PRF_INCOMING_FLIT_GBL	RT_FLIT_GBL	Total number of flits received on all global links of a router
AR_RTR_INQ_PRF_ROWBUS_STALL_ROW	RT_STL_ROW	Total number of stalls on all row links of a router
AR_RTR_INQ_PRF_ROWBUS_STALL_COL	RT_STL_COL	Total number of stalls on all column links of a router
AR_RTR_INQ_PRF_ROWBUS_STALL_GBL	RT_STL_GBL	Total number of stalls on all global links of a router
AR_NL_PRF_REQ_FLITS	PT_FLIT_REQ	Total number of NIC request flits on a processor tile
AR_NL_PRF_RSP_FLITS	PT_FLIT_RSP	Total number of NIC response flits on a processor tile
AR_NL_PRF_REQ_STALLED	PT_STL_REQ	Total number of cycles requests stalled on a processor tile
AR_NL_PRF_RSP_STALLED	PT_STL_RSP	Total number of cycles responses stalled on a processor tile

all router tiles yields the 17 (2×8 VCs + row_bus stalls) counters derived from the top section of Table I. A similar reduction across all the processor tiles yields derived counters corresponding to the bottom section of Table I. After this reduction, we are left with $17 + 8 = 25$ derived features for each of the 2,890 routers for each job run in our dataset.

Creating Interpretable Derived Features: Next, we perform a sum over different virtual channel groups to create a set of human interpretable derived features (Table II). For example,

$$\text{AR_RTR_INQ_PRF_INCOMING_FLIT_REQ} = \sum_{v=0}^3 \text{AR_RTR_INQ_PRF_INCOMING_FLIT_VC}_v \quad (1)$$

$$\text{AR_RTR_INQ_PRF_INCOMING_FLIT_RSP} = \sum_{v=4}^7 \text{AR_RTR_INQ_PRF_INCOMING_FLIT_VC}_v \quad (2)$$

In the equations above, v is the virtual channel number that appears in the column names in the first two rows of Table I. There are eight virtual channels and v iterates over the virtual channel ID (0 to 3 in Equation 1, and 4 to 7 in Equation 2).

Such groupings lead to the top section of Table II). Similarly $\text{AR_NL_PRF_REQ_NIC_n_TO_PTILES_FLITS}$ and $\text{AR_NL_PRF_REQ_PTILES_TO_NIC_n_FLITS}$ for a processor tile are summed together to create the $\text{AR_NL_PRF_REQ_FLITS}$ feature (bottom section of Table II). The colors in Table I and II provide a mapping between the raw and derived features. The middle section of Table II represents another way of creating derived features. Instead of reducing counters over all router tiles, we reduce the flit and stall counters by the type of port or link (row, column, or global). This creates the six features in the middle section of Table II. These different derivations yield 14 derived features for each of the 2,890 routers.

Filtering by Router Type: Different types of nodes such as compute nodes, I/O servers, management and login nodes are

attached to different routers. We can either consider all routers or filter the data by the types of nodes attached to a router. We explored the following groupings, each of which only considers a subset of routers: routers connected to compute nodes (henceforth referred to as *all routers*), routers connected to I/O servers (*IO routers*), and routers attached to nodes that are assigned to the control job (henceforth referred to as *my routers*). These three groupings yielded the strongest results in our experiments, and are solutions that can be implemented by system administrators and individual users respectively.

Aggregating over Routers: For each grouping described above, we explored various schemes to aggregate the data across routers for the set of derived features. This aggregation calculates one value for each feature by applying one of the following functions over all the routers that belong to a group: mean, standard deviation, various percentiles such as median, 75th percentile, 95th percentile, and IQR (75th – 25th percentile). We present results for some of these aggregation functions in Section V.

C. Control Jobs Data

We set up some control jobs that enable us to assess the impact of system state on the performance of production applications. We run three codes – AMG, MILC, and miniVite, which are representative of common workloads on HPC systems. AMG and MILC were run in a weak scaling mode on 128 and 512 nodes. miniVite’s input problem is a fixed-size real world graph, and it was only run on 128 nodes. Each application run was short, running for between five to ten minutes. We briefly describe each application below.

AMG: is a proxy application for parallel algebraic multigrid and it uses the Hypr linear solver library [21]. In our setup, AMG runs AMG-GMRES on a linear system for a three-dimensional input problem with dimensions $32 \times 32 \times 32$ (per MPI process).

MILC: refers to MIMD Lattice Computation, used for numerical simulations of quantum chromodynamics. The MILC

application, `su3_rmd`, was used in these experiments, which performs a 4D stencil on a per process grid of dimensions $4 \times 4 \times 4 \times 4$.

miniVite: is a proxy application for Vite [22], and is representative of graph analytics workloads [23]. It performs a single phase of the Louvain classification, which is an algorithm for community detection in large distributed graphs. An iterative loop was added to miniVite to repeat its work several times.

Data for experiments in this paper was collected by submitting control jobs for each application to the production batch queue on Cori between December 2018 and April 2019. All control jobs were run on KNL nodes, alongside jobs of other users on the system. Four out of 68 cores on each node were reserved for OS daemons to minimize the effects of OS noise on compute regions in the code. The applications did not perform any I/O, to rule out variability due to I/O congestion. Based on when each job ran, LDMS data was processed to obtain the derived features for the 5-minute interval prior to the execution of the job (Figure 3). We also recorded the execution time for the main execution loop of each application, which is the variable the ML models try to predict. Table III presents the five datasets created for training the models and the number of samples in each dataset. Note that whenever we refer to an application dataset in the paper, it refers to the system-wide data collected from the 5-minute interval prior to the beginning of each job in the dataset and that job’s respective execution time. The models are trained solely on the system-wide data and no application-specific data is used for training.

TABLE III
DATASETS BASED ON APPLICATIONS RUN IN THE CONTROL JOBS

Application	No. of Nodes	Number of jobs	Dataset Name
AMG 1.1	128	156	AMG 128
AMG 1.1	512	152	AMG 512
MILC 7.8.0	128	151	MILC 128
MILC 7.8.0	512	153	MILC 512
miniVite 1.0	128	119	miniVite

Job Placement Data: We also calculate two additional job-related features from scheduler queue logs. The first, `NUM_ROUTERS`, indicates the total number of unique routers that a job was assigned nodes on. The second, `NUM_GROUPS`, indicates how many dragonfly groups these routers were spread across. These features indicate the degree of compactness or spread in terms of placement of each job.

IV. METHODS FOR DATA ANALYTICS

In this section, we present our approach for creating prediction models, obtaining importance of different features, and evaluating the predictive power of the trained models.

A. Machine Learning based Prediction Models

We use a Gradient Boosting regressor (GBR) both as our prediction model, and for assigning importances to input features. GBRs utilize an ensemble method that assumes that

the true regression function is a linear combinations of several different base learners [24], [25]. These base learners typically constitute decision trees, which have the benefit of higher levels of human interpretability particularly in determining the importances of input features. Since the number of samples per application dataset is relatively small, we solely consider GBR in our experiments to determine feature importances.

In addition to using GBR, we also train a neural network when combining multiple datasets to create application-agnostic models in Section V-C. The larger combined dataset allows for more complex models. We utilize a small neural network consisting of two 8-node hidden layers each with a 50% dropout connected to a final output layer with a linear activation. The dropout layers randomly select 50% of the nodes to exclude from a layer during training and help to reduce overfitting [26]. GBRs can struggle with extrapolation so a neural network was selected to counter this specificity [27].

B. Training the Models

In Sections V-A and V-B, we train separate machine learning models for each of the first four datasets in Table III. We perform a 20-fold cross-validation, where the dataset is split into 20 parts randomly. One part is reserved for testing and the other 19 parts are used for training. The inputs to the ML algorithms for creating the dataset-specific ML models are: (1) for each sample (job) in the training set, values of the counters described in Table II for the five minutes prior to the start of that job are provided as the input features, and (2) execution time of each sample (job) is provided as the dependent variable to be modeled. Given a set of samples in the testing set, the model outputs the predicted execution time of each testing sample based on the values of the independent features (counter values) for that sample. We standardize all input features (counter values) and the execution time of the training data (yielding a mean of zero and standard deviation of one for each feature and the output vector). When testing a model, we apply the same standardization vectors obtained from the training data on the test data.

In Section V-C, we create an application-agnostic model that can predict the performance of an arbitrary application not included in the training dataset. We create multiple training datasets by combining data samples from different rows of Table III, and leaving some samples for testing entirely. For example, in one instance, we combine the following three datasets – AMG 128, AMG 512, and MILC 128, train a model using the combined data, and use the trained model to predict the performance of MILC 512. In a separate study, we combine datasets by application type. For example, we combine all AMG and MILC datasets, train a model, and use miniVite as an unseen testing dataset. Note that when we combine multiple datasets, we standardize their features and execution times separately. We de-normalize the output by using a standardization vector created from the oracle execution times of the testing data. If we were to use such a model for a new application, we would not have a standardization vector for de-normalizing the predicted values. However, the standardized

output still allows analyzing relative expected performance, and provides a strong heuristic for overall runtime with only an estimation of the true application runtime distribution.

C. Calculating Feature Importances

To evaluate the relative importances of the derived system-wide counters in forecasting job runtime, we use the technique of recursive feature elimination (RFE). For each application dataset, we perform a summary across a particular router type using an aggregation function, and train a GBR model. scikit outputs importances of each feature, where the importance is computed as the (normalized) total reduction of the mean squared error brought by that feature. It is also known as the Gini importance. We identify the worst performing feature based on feature importances, drop that feature from the training data, and train again with the smaller set of features. This process continues until all features are eliminated. Finally, we create a ranking based on when each feature is eliminated, and use this ranking to select the five best features and compute a relevance score for each.

We use a tree-based feature importance metric for the GBR. For each feature utilized by each of GBR's decision trees, the total reduction in mean squared error that can be attributed to a branch utilizing that feature is calculated for all features [28]. Note that all input features in our dataset are strictly numeric and thus less susceptible to biases sometimes present in tree-based feature importances. For each dataset, we perform this calculation of feature importances 5-fold and average the results across all validation splits.

D. Metrics for Evaluation

We define two metrics that are indicative of the quality of predictions w.r.t. overall job runtime. The first, mean absolute percentage error (MAPE), calculates the mean of percentage errors observed for each test sample as follows,

$$\text{MAPE} = \frac{1}{n} \sum_i^n \frac{|y_i - \hat{y}_i|}{y_i}$$

where, y_i is the true value, \hat{y}_i is the predicted value, and n is the number of samples in the dataset.

We also define an additional metric to measure the relative accuracy of our regression models: percent of samples with large error (PSLE). We define a test sample to have a large error if the predicted value is more than $x\%$ higher or lower than its true value. For a dataset, PSLE is defined as,

$$\text{PSLE} = \frac{1}{n} \sum_{i=1}^n LE_i$$

$$LE_i = \begin{cases} 1, & \text{if } \frac{|y_i - \hat{y}_i|}{y_i} > x \\ 0, & \text{otherwise} \end{cases}$$

We use $x = 0.15$ for the evaluation in this paper. This metric is important because when a system wants to use the model, it may not need exact predictions of the job runtime. It may be more important to predict the general trend i.e. is the next job going to run reasonably fast or unreasonably slow? We

chose $x = 0.15$ because if the ML model is mis-predicting by more than 15%, then the job scheduler should probably not use the results to decide if the job will run slow or fast. We use MAPE and PLSE as opposed to the standard ML metrics because they provide a more intuitive understanding of the efficacy of the model for the HPC performance domain.

V. EVALUATION OF TRAINED ML MODELS

We now evaluate and compare the prediction models trained on different datasets and their combinations, for different router groupings and aggregation functions.

A. Models based on Different Router Groups

In order to understand the significance of different router groups in predicting performance, we created GBR models for each application dataset using three different router groups – my routers, IO routers, and all compute routers. We observe that despite a small number of samples per application dataset, all models perform sufficiently well (Figure 4). All router groups are good at predicting AMG performance with MAPE below 5% and for MILC, which has a much higher variance in runtime, all MAPEs are below 10%. The All routers grouping is somewhat better than the other two. We see a similar trend with the Percentage Samples with Large Error (PSLE) metric — for AMG, the models predict worse than 15% for less than 5% of the test data. However, for MILC, PSLE is somewhat higher due to the high variability in the MILC dataset. We also observe that we obtain good scores for both My routers and All routers groupings. This indicates that both system administrators and individual HPC users could achieve similar success in predicting complex job execution with small amount of temporal information.

Using recursive feature elimination for both AMG and MILC datasets, we calculate relative importance scores for all input features in the My routers and All routers groupings. Figure 5 visualizes the importances of the derived features for the four datasets (each row is for one dataset). We observe that the two router groupings rely on some common features – RT_PKT_RSP (stalls on router tiles), RT_STL_GBL (stalls on global links), PT_FLIT_REQ (processor tile flits), and PT_STL_RSP (processor tile stalls). It is not surprising that job performance depends on stalls on router and processor tiles, specifically on stalls on global links. For both applications, performance also depends on the number of flits sent on processor tiles.

B. Models by Different Types of Aggregation

In the previous section, we used the mean function to aggregate data over all routers in a particular group. We now consider several other aggregation strategies, and the top performing aggregations for the all routers grouping are shown in Figure 6. We observe that across these top performing aggregation schemes, the prediction scores do not vary significantly for the different applications. In terms of the application of these prediction models in a system-wide job scheduler, we see this as a promising result as the true mean across all routers

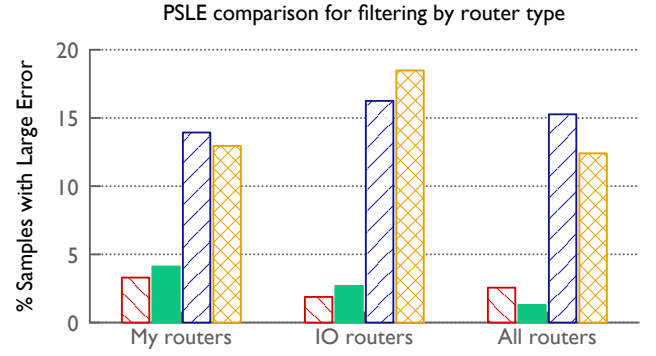
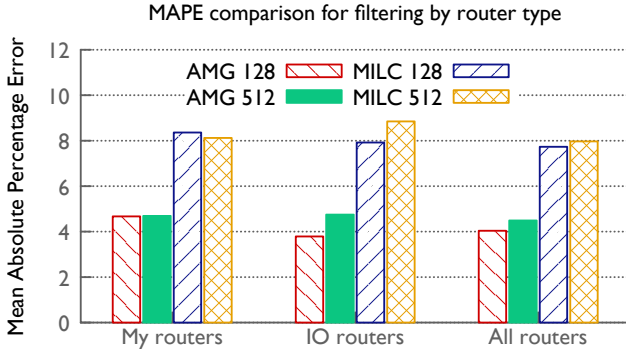


Fig. 4. MAPE and PSLE scores for the GBR model when using different router types for filtering the system-wide data.

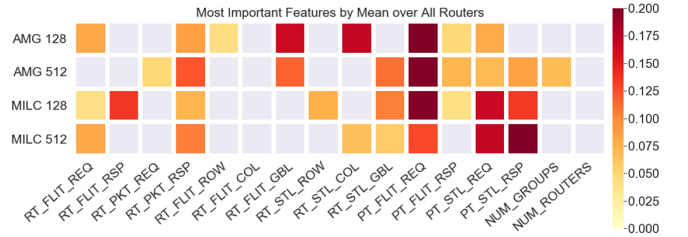
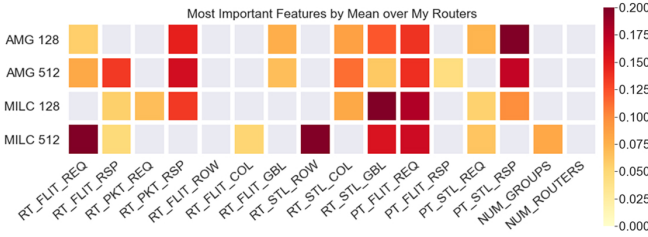


Fig. 5. Relative importances of the most important counters obtained using RFE for different datasets (aggregation function: mean).

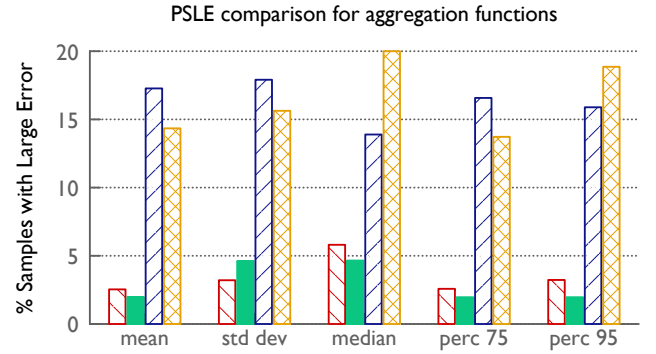
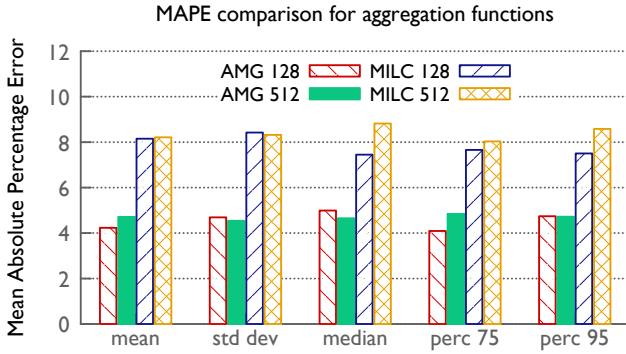


Fig. 6. MAPE and PSLE scores for the GBR model when using different aggregation functions over all compute routers.

is not needed. It highlights the potential for strong results using a computationally less-expensive aggregation and for accurate estimation using a small subset of routers.

Next, we perform RFE on the derived features when using the 75th percentile function for aggregation. Figure 7 shows the feature importances for the 75th percentile aggregation over the All routers grouping. We see a consistent story in the feature importances to the mean aggregation (Figure 5) suggesting a robustness in this ranking strategy. Some of the same derived counters appear to be the most important – RT_STL_GBL (stalls on global links), PT_FLIT_REQ (processor tile flits), and PT_STL_RSP (processor tile stalls). RT_PKT_RSP (stalls on router tiles) appears to be less impor-

tant now but some other features also appear to be important in this scenario: RT_FLIT_REQ (router tile flits), RT_STL_ROW (stalls on row links), and PT_STL_RSP (processor tile stalls).

C. Application-agnostic Models

Finally, we analyze the generalizability of the ML algorithms and their prediction models. Generalization refers to a model's ability to adapt to new unseen data. When we reserve an entire application for testing and do not include it in training, and repeat this with different applications, it tests the generalizability of the model. The end goal is to train a single model that can accurately predict the standardized runtime for any application even if we do not have data for that application

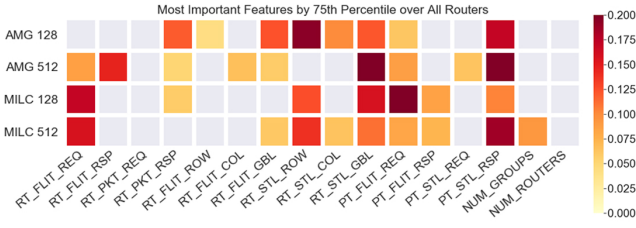


Fig. 7. Relative importances of the most important counters obtained using RFE for different datasets (router grouping: all routers).

in the training dataset. In the first study of generalizability, we use four datasets – AMG 128, AMG 512, MILC 128, and MILC 512. In turns, we use three of these datasets for training and reserve the fourth dataset entirely for testing. We segment the training data into 8-fold cross-validation segments and train a model that can predict the standardized runtime of any job in the testing set given the previous five minutes of system data. Each prediction is later de-normalized with respect to its application and an error metric is calculated for that prediction. For all the results in this section, we use the neural network model, apply the mean function to aggregate the data, and compare using the All routers versus My routers data.

Figure 8 shows the success of the trained models in terms of their MAPE and PSLE scores. Comparing with Figure 6, we observe that when multiple datasets are combined for training, the models perform better in terms of predicting the execution times, compared to training on a portion of the individual datasets by themselves. The MAPE for predicting AMG 128 reduces from 4.23 to 3.61 and that for AMG 512 from 4.71 to 4.25. Similarly the MAPE for predicting MILC 512 reduces from 8.21 when used by itself for training to 7.5 when the other three datasets are combined for training a model. This improvement is likely due to the larger training dataset (~450 samples versus ~150) allowing for more robust training of models. We see this as a promising sign for future models which could include tens of applications with hundreds of samples each and likely even stronger and more generalizable predictions. We also observe that using the data from only the routers allocated to a job does not degrade the models significantly. This suggests that in absence of system-wide data, an end user can use data from the routers that they have access to via their jobs.

In the second study of generalizability, we combine datasets by application type and reserve one of the applications as unseen data for testing. For example, when we combine all AMG and MILC datasets for training, we use the miniVite dataset for testing. Figure 9 shows how these application-agnostic models perform in terms of predicting the performance of an unseen application. We observe that AMG has the lowest errors, followed by MILC and then miniVite. On average, AMG has the lowest percentage of communication with respect to its total execution time, followed by MILC, and then miniVite. As a result, AMG has the lowest performance variability and miniVite the highest. We believe that this is the reason for the

models performing better in predicting AMG’s performance as opposed to that of MILC and miniVite. Nevertheless, the results are still encouraging. Even without any data for an application being included in the training dataset, the ML models exhibit reasonable success in performance prediction. We expect that adding more applications with different computation and communication signatures to our training dataset will improve the prediction scores for unseen applications.

Finally, we analyze feature importances when training the neural network model using the combined datasets. Figure 10 shows the relative feature importances for three different training datasets (AMG+MILC, AMG+miniVite, and MILC+miniVite), and two filterings (All routers and My routers). Surprisingly, NUM_GROUPS emerges as a highly important feature. In theory, one would expect that the placement of a job should have little impact on its performance due to adaptive indirect (UGAL) routing [9]. However, in practice, it is possible that when a job is spread over more groups, the likelihood of encountering congestion on global links increases. RT_STL_GBL (stalls on global links) is also important for predicting all three applications as we had observed in the previous plots. We also observe that while applications share common important features, some features are only important for certain datasets. We notice that PT_STL_REQ (processor request stalls) is more important when training using the AMG+miniVite dataset. A feature that is important when filtering by My routers but not All routers is RT_STL_COL (stalls on black links). On the other hand, RT_FLIT_REQ (router request flits) is important when filtering by All routers.

VI. INFLUENCING JOB SCHEDULING DECISIONS

We now discuss how the findings in previous sections could be used by a job scheduler or HPC user for labeling incoming jobs in the queue as likely to run relatively fast or slow. The hypothesis is that by selecting a small number of features (network counters) based on feature importances, and analyzing their values when a new job is ready to be scheduled, the job scheduler can quickly determine if the job will run slow or fast. If this succeeds, a job scheduler can decide to monitor certain features continuously, based on feature importances derived from the application-agnostic models in Section V-C.

We select the three most important features from the application-agnostic models in Figure 10: NUM_GROUPS, RT_STL_GBL, and RT_STL_COL. Next, we classify samples (jobs) in three of our datasets (AMG 512, MILC 512, and miniVite 128) as “likely fast” or “likely slow” based on whether the system-wide values of these three counters in the five minutes prior to that job running were below or above the median of all observed values respectively. Once the jobs in a dataset have been classified into likely fast or slow based on the values of the selected network counters, we analyze their actual execution times (ground truth) to check if our classification is statistically significant.

Figure 11 shows the distributions of the execution times of the likely fast and slow sets of jobs in the MILC 512 dataset. The histograms were generated with a fixed number of bins

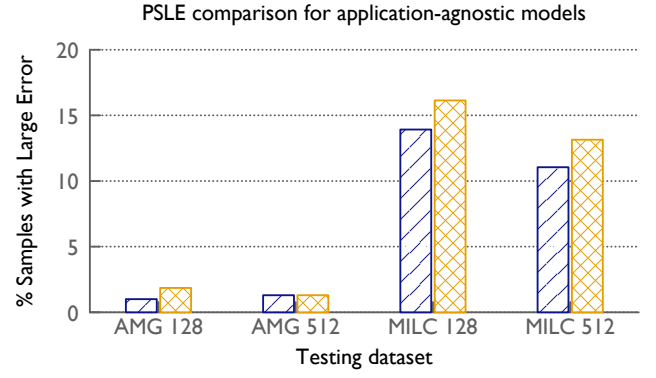
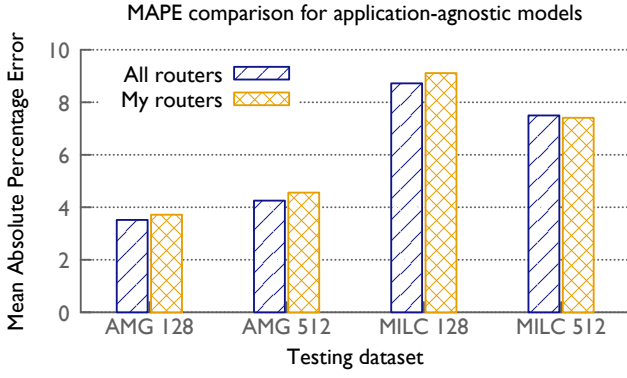


Fig. 8. MAPE and PSLE scores for the NN model when using three datasets for training and a fourth disjoint dataset for testing (x-axis label.) The training dataset for each cluster is the combination of AMG 128, AMG 512, MILC 128, MILC 512 minus the dataset in the x-axis label.

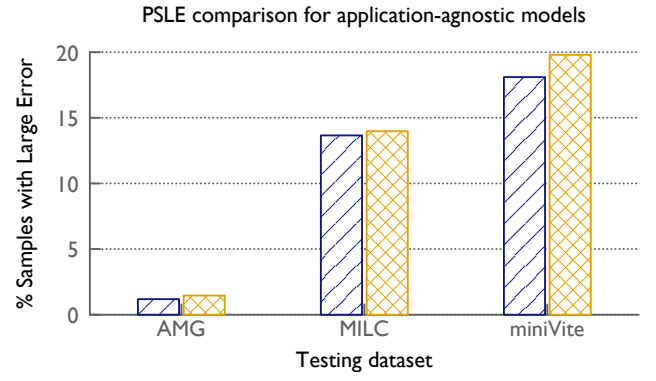
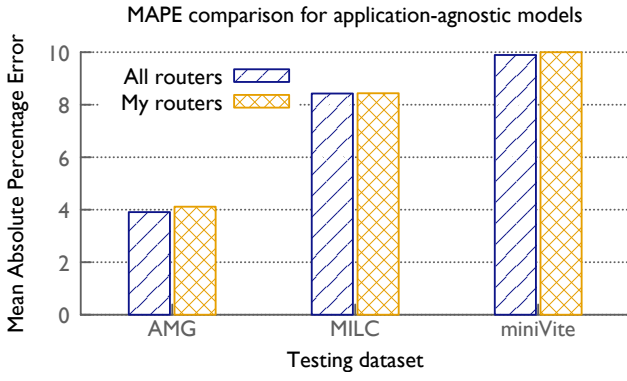


Fig. 9. MAPE and PSLE scores for the NN model when combining datasets by application type. Two applications are used for training and the third application is used for testing (x-axis label.)

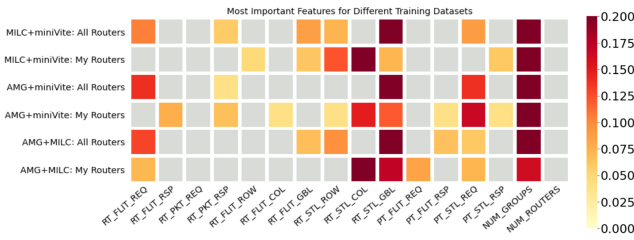


Fig. 10. Relative importances of the most important counters obtained using RFE for different router groups in the application-agnostic model.

over the entire execution time range of a given dataset. Given the right skew present in application runtimes, we elected to use the Kruskal-Wallis H. Test to test for a difference in medians between the runtimes of likely fast and slow jobs in each application dataset. We found that for all the applications, the calculated p-value was below $3e-05$, indicating a statistically significant difference between the likely fast and slow execution times. Note that a one-way ANOVA test yields statistically significant results below the 1% threshold for all applications. Table IV compares the mean execution times of

the likely fast versus slow jobs in each dataset. We can see that the difference is significant, especially for MILC and miniVite in spite of their predictions being poorer than AMG. This is a powerful result with significant implications for improving application performance and reducing variability.

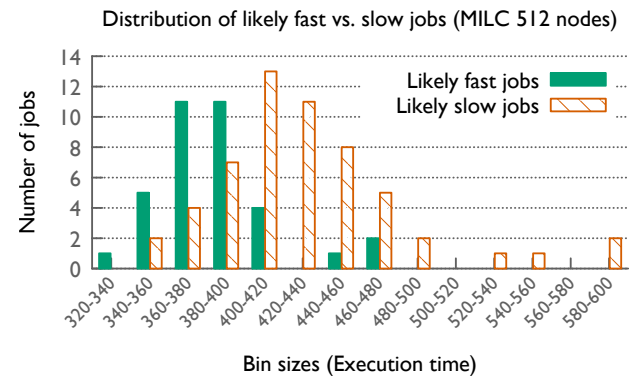


Fig. 11. Distribution of actual runtimes of likely fast versus slow jobs of MILC when considering above median values of three features: RT_STL_COL, RT_STL_GBL, and NUM_GROUPS

TABLE IV
MEAN EXECUTION TIMES (IN SECONDS) OF THE LIKELY FAST AND SLOW
SUBSETS OF JOBS IN EACH DATASET

Application	Fast jobs	Slow jobs
AMG 128	260.12	274.24
AMG 512	379.93	410.68
MILC 128	317.31	398.43
MILC 512	389.61	445.80
miniVite 128	309.96	372.26

We foresee two immediate applications of such a system. Many HPC systems set an upper bound on the time requested for a job (12 or 24 hours). As a result, science simulations requiring months of running time must be submitted as multiple jobs to the job queue periodically. While the inputs may change somewhat as computation progresses, the overall runtime profile and networking requirements of an application usually do not vary significantly, providing an optimal use case for our prediction system. When a job gets scheduled, individual HPC users can gather network counter data for a few minutes on all the routers assigned to their job and use our pre-trained models to predict the expected runtime of their application. They can use this prediction to decide whether to go ahead with launching their application or to give the allocation back and request another job later when the system is less congested.

Second, these results suggest that an intelligent job scheduler can monitor a handful of counters, and use their current values to determine if, for example, communication-heavy jobs will perform well or poorly if scheduled right away. Figure 11 demonstrates the power of predicting job execution time solely based on the median aggregation of just three network counters. While in this paper, we analyzed these jobs after they had run, a job scheduler would have access to similar counter data through LDMS at the time when a job is ready to be scheduled. Such adaptive decisions based on light-weight monitoring of a few hardware counters on a subset of routers could prove to be immensely useful.

VII. SUMMARY AND FUTURE WORK

In summary, we presented a data analytics study of longitudinal system-wide monitoring data to predict the performance of unseen jobs pending in the scheduler queue. We presented a pipeline for extracting relevant data from a time series, creating interpretable derived features, reducing the data, and filtering and aggregating it in meaningful ways. We then created several prediction models that only look at prior system state before a job starts executing to predict its runtime. Our models performed well on two different metrics and also helped in identifying important input features. We then demonstrated the use of three network hardware counters to classify jobs in a dataset into likely fast and likely slow with statistically significant results. This demonstrates that an intelligent job scheduler could use a similar simple mechanism to forecast the performance of a pending job. Our proposed pipeline and

analysis remain relevant across different HPC systems and routers as our work can be applied to any system with LDMS data collection.

In the future, we plan to perform more detailed analysis of system- and facility-wide monitoring data to detect patterns and anomalies in it. We also plan to create a large library of performance datasets that can be used to train machine learning models that would be successful in predicting the performance of any new code. We also plan to modify existing job scheduling algorithms to incorporate machine learning models for making real-time decisions that reduce performance variability.

ACKNOWLEDGMENT

This material is based upon work supported in part by the National Science Foundation under Grant No. 2047120.

REFERENCES

- [1] F. Petrini, D. J. Kerbyson, and S. Pakin, "The Case of the Missing Supercomputer Performance: Achieving Optimal Performance on the 8,192 Processors of ASCI Q," in *Proceedings of the 2003 ACM/IEEE conference on Supercomputing (SC'03)*, 2003.
- [2] A. Bhatele, K. Mohror, S. H. Langer, and K. E. Isaacs, "There goes the neighborhood: performance degradation due to nearby jobs," in *Proceedings of the ACM/IEEE International Conference for High Performance Computing, Networking, Storage and Analysis*, ser. SC '13. IEEE Computer Society, Nov. 2013. [Online]. Available: <http://doi.acm.org/10.1145/2503210.2503247>
- [3] A. Bhatele, J. J. Thiagarajan, T. Groves, R. Anirudh, S. A. Smith, B. Cook, and D. K. Lowenthal, "The case of performance variability on dragonfly-based systems," in *Proceedings of the IEEE International Parallel & Distributed Processing Symposium*, ser. IPDPS '20. IEEE Computer Society, May 2020.
- [4] G. K. Lockwood, S. Snyder, T. Wang, S. Byna, P. Carns, and N. J. Wright, "A year in the life of a parallel file system," in *Proceedings of the International Conference for High Performance Computing, Networking, Storage, and Analysis*, ser. SC '18. IEEE Press, 2018.
- [5] D. Nichols, A. Marathe, K. Shoga, T. Gambelin, and A. Bhatele, "Resource utilization aware job scheduling to mitigate performance variability," in *Proceedings of the IEEE International Parallel & Distributed Processing Symposium*, ser. IPDPS '22. IEEE Computer Society, May 2022.
- [6] A. Agelastos, B. Allan, J. Brandt, P. Cassella, J. Enos, J. Fullop, A. Gentile, S. Monk, N. Naksinehaboon, J. Ogden, M. Rajan, M. Showerman, J. Stevenson, N. Taerat, and T. Tucker, "The lightweight distributed metric service: A scalable infrastructure for continuous monitoring of large scale computing systems and applications," in *SC '14: Proceedings of the International Conference for High Performance Computing, Networking, Storage and Analysis*, 2014, pp. 154–165.
- [7] A. Agelastos, B. Allan, J. Brandt, A. Gentile, S. Lefantzi, S. Monk, J. Ogden, M. Rajan, and J. Stevenson, "Continuous whole-system monitoring toward rapid understanding of production hpc applications and systems," *Parallel Computing*, vol. 58, pp. 90 – 106, 2016. [Online]. Available: <http://www.sciencedirect.com/science/article/pii/S0167819116300394>
- [8] J. Kim, W. J. Dally, S. Scott, and D. Abts, "Technology-driven, highly-scalable dragonfly topology," in *2008 International Symposium on Computer Architecture*. IEEE Computer Society, 2008.
- [9] A. Singh, "Load-balanced routing in interconnection networks," Ph.D. dissertation, Dept. of Electrical Engineering, Stanford University, 2005, http://cva.stanford.edu/publications/2005/thesis_arjuns.pdf.
- [10] T. Hoefler, T. Schneider, and A. Lumsdaine, "Characterizing the influence of system noise on large-scale applications by simulation," in *Proceedings of the 2010 ACM/IEEE International Conference for High Performance Computing, Networking, Storage and Analysis*, ser. SC '10. USA: IEEE Computer Society, 2010. [Online]. Available: <https://doi.org/10.1109/SC.2010.12>

- [11] T. Groves, Y. Gu, and N. J. Wright, "Understanding performance variability on the aries dragonfly network," in *2017 IEEE International Conference on Cluster Computing (CLUSTER)*, 2017, pp. 809–813.
- [12] R. Wolski, N. Spring, and C. Peterson, "Implementing a performance forecasting system for metacomputing: The network weather service," in *Proceedings of the 1997 ACM/IEEE Conference on Supercomputing*, ser. SC '97. New York, NY, USA: Association for Computing Machinery, 1997. [Online]. Available: <https://doi.org/10.1145/509593.509600>
- [13] D. Skinner and W. Kramer, "Understanding the causes of performance variability in hpc workloads," in *Workload Characterization Symposium, 2005. Proceedings of the IEEE International*. IEEE, 2005, pp. 137–149.
- [14] O. Tuncer, E. Ates, Y. Zhang, A. Turk, J. Brandt, V. J. Leung, M. Egele, and A. K. Coskun, "Online diagnosis of performance variation in hpc systems using machine learning," *IEEE Transactions on Parallel and Distributed Systems*, vol. 30, pp. 883–896, 2019.
- [15] D. Hoppe, L. Zhong, S. Andersson, and D. Moise, "On the detection and interpretation of performance variations of hpc applications," in *Sustained Simulation Performance 2018 and 2019*, M. Resch, Y. Kovalenko, W. Bez, E. Focht, and H. Kobayashi, Eds. Springer, 03 2020, pp. 41–56.
- [16] S. Jha, J. Brandt, A. Gentile, Z. Kalbarczyk, and R. Iyer, "Characterizing supercomputer traffic networks through link-level analysis," in *2018 IEEE International Conference on Cluster Computing (CLUSTER)*, Sep. 2018, pp. 562–570.
- [17] S. Chunduri, K. Harms, S. Parker, V. Morozov, S. Oshin, N. Cherukuri, and K. Kumaran, "Run-to-run variability on xeon phi based cray xc systems," in *Proceedings of the International Conference for High Performance Computing, Networking, Storage and Analysis*, ser. SC '17. New York, NY, USA: ACM, 2017.
- [18] S. Chunduri, E. Jennings, K. Harms, C. Knight, and S. Parker, "A generalized statistics-based model for predicting network-induced variability," in *2019 IEEE/ACM Performance Modeling, Benchmarking and Simulation of High Performance Computer Systems (PMBS)*, 2019, pp. 59–72.
- [19] "Cori system." [Online]. Available: <https://docs.nersc.gov/systems/cori/>
- [20] "Aries hardware counters (s-0045-20)," <http://docs.cray.com/books/S-0045-20/S-0045-20.pdf>, 2017.
- [21] R. Falgout, J. Jones, and U. Yang, "The design and implementation of hypre, a library of parallel high performance preconditioners," in *Numerical Solution of Partial Differential Equations on Parallel Computers*, A. Bruaset and A. Tveito, Eds. Springer-Verlag, 2006, vol. 51, pp. 267–294.
- [22] S. Ghosh, M. Halappanavar, A. Tumeo, A. Kalyanaraman, H. Lu, D. Chavarrià-Miranda, A. Khan, and A. Gebremedhin, "Distributed louvain algorithm for graph community detection," in *2018 IEEE International Parallel and Distributed Processing Symposium (IPDPS)*, May 2018, pp. 885–895.
- [23] S. Ghosh, M. Halappanavar, A. Tumeo, A. Kalyanaraman, and A. H. Gebremedhin, "Minivite: A graph analytics benchmarking tool for massively parallel systems," in *2018 IEEE/ACM Performance Modeling, Benchmarking and Simulation of High Performance Computer Systems (PMBS)*, Nov 2018, pp. 51–56.
- [24] Y. Freund, R. Iyer, R. E. Schapire, and Y. Singer, "An efficient boosting algorithm for combining preferences," *Journal of machine learning research*, vol. 4, no. Nov, pp. 933–969, 2003.
- [25] J. H. Friedman, "Greedy function approximation: A gradient boosting machine," *The Annals of Statistics*, vol. 29, no. 5, pp. pp. 1189–1232, 2001.
- [26] N. Srivastava, "Improving neural networks with dropout," *University of Toronto*, vol. 182, no. 566, p. 7, 2013.
- [27] P. Prettenhofer and G. Louppe, "Gradient boosted regression trees in scikit-learn," 2014.
- [28] M. Sandri and P. Zuccolotto, "Analysis and correction of bias in total decrease in node impurity measures for tree-based algorithms," *Statistics and Computing*, vol. 20, no. 4, pp. 393–407, 2010.